

Effect of Radiation Drag on Hoyle-Lyttleton Accretion

Tomomi NIO,^{1*} Takuya MATSUDA,¹ and Jun FUKUE²

¹ *Department of Earth and Planetary Sciences, Kobe University, Kobe 657-8501*

² *Astronomical Institute, Osaka Kyoiku University, Asahigaoka, Kashiwara, Osaka 582-8582*

E-mail(TN): nio@stp.isas.ac.jp

* Present address: The Institute of Space and Astronautical Science, Yoshinodai, Sagamihara, Kanagawa 229-8510 and Department of Earth and Planetary Physics, University of Tokyo, Hongo, Bunkyo-ku, Tokyo 113-8654

Abstract

Hoyle-Lyttleton type accretion is investigated, by taking account of not only the effect of radiation pressure but the effect of radiation drag. We calculate the trajectories of particles for three cases: only the effect of gravity is considered (case A); the effect of radiation pressure is taken into account (case B); the effect of radiation drag as well as radiation pressure is taken into account (case C). The accretion radii for former two cases are $2GM/v_\infty^2$ for case A and $2GM(1 - \Gamma)/v_\infty^2$ for case B, where M is the mass of the accreted object, v_∞ the relative velocity, and Γ the normalized luminosity of the accreted object. We found that the accretion radius for case C is in between those of cases A and B under the present approximation; i.e., the accretion radius decreases due to radiation pressure while it increases due to radiation drag. In addition, the accretion radius for case C becomes larger as the incident velocity becomes fast. The effect of radiation drag becomes more and more important when the velocity of the incident particle is comparable to the light speed.

Key words: Accretion — Accretion disks — Radiation: mechanisms — X-rays: binaries

1. Introduction

Accretion is a phenomenon, in which gas is attracted by a gravitating astrophysical object and accretes on it. In this process potential energy is liberated, and the accreting gas becomes hot and emits radiation. If the accreted body is a compact object such as a neutron star or a black hole, significant fraction of the rest mass energy of the accreting gas is liberated, and the efficiency of energy conversion exceeds that of nuclear energy. Thus, the accretion process can be a major source of energy in astrophysics.

In the simplified model of the axisymmetric accretion introduced by Hoyle and Lyttleton (1939), the field of a gravitating body acts on surrounding streams of particles, which has a uniform flow upstream at infinity. These particles move on hyperbolic orbits, which intersect downstream of the point mass on the axis of symmetry (the accretion axis). Pressure forces are everywhere neglected, although the intersecting particles are allowed to collide and coalesce on the accretion axis. Particles colliding close enough to the point mass lose enough of their kinetic energy to be trapped by the central object.

Bondi and Hoyle (1944) replaced the infinitely-thin accretion axis by a broader accretion column, in which pressure forces play a role (see also Davis, Pringle 1980). Bondi (1952) also considered a spherical accretion without bulk motion of a gravitating object, taking account of the gas pressure (see Treves et al. 1988 for a review). In the Hoyle-Lyttleton type accretion the effect of gas pressure is taken into account numerically by several researchers (Hunt 1971; Shima et al. 1985; Fryxell et al. 1987; Ho et al. 1989; Koide et al. 1991). In these calculations, however, the effect of radiation pressure was neglected. The effect of radiation pressure was taken into account by, e.g., Taam et al. (1991). Due to radiation pressure, the accretion radius and the accretion rate are significantly reduced from the Hoyle-Lyttleton estimate.

In these studies they have neglected the effect of *radiation drag* (such as Compton drag). In the ionized gas the radiation drag force becomes important if the velocity of gas is comparable to the light speed and the luminosity of the central object is comparable to the Eddington luminosity. Since such a condition was supposed to be rarely fulfilled in realistic astrophysical situations, the effect of radiation drag has been neglected so far. Radiation drag is also important, if the specific cross-section — “opacity” — of particles is sufficiently large like, e.g., dust.

Of course, since the discovery of Poynting-Robertson effect (Poynting 1903; Robertson 1937), the effect of radiation drag on particles moving around the radiating object has been studied by several authors. For example, Guess (1962) examined the Poynting-Robertson effect for the case of a finite spherical source. He also examined the particle trajectories in details. Carroll (1990) also examined the Poynting-Robertson effect more generally. In the field of accretion disks, furthermore, the effect of radiation drag was extensively investigated recently, since in the inner region of accretion disks the radiation field is so intense and the rotation velocity is so high that radiation drag becomes important (see, e.g., Fortner et al. 1989; Meyer, Meyer-Hofmeister 1994; Fukue, Umemura 1995; Tajima, Fukue 1996; Watanabe, Fukue 1996; see also Kato et al. 1996).

In Hoyle-Lyttleton type accretion, the effect of radiation drag has not been considered yet. However, there can be a situation in which a luminous source moves at a high velocity and radiation drag becomes important. For example, in the case of supernova explosions a neutron star can be ejected from a binary system at a high speed comparable to the light speed. In compact binaries a neutron star or a black hole surrounded by accretion disks, which rotates at a high orbital velocity, can feed gas from companion winds. In astrophysical jets, whose speed is of the order of the light speed, a gravitating object can be located in the jet flow. Moreover, since the effect of radiation drag is a fundamental process in astrophysics, it is worthwhile to investigate it.

In the next section we describe an axisymmetric accretion, the radiation fields, and the basic equations. Numerical results are presented in section 3. Final section is devoted to the concluding remarks.

2. Model

2.1. Hoyle-Lyttleton Axisymmetric Accretion

As we discussed in the introduction, the axisymmetric accretion is modeled as follow. Let us suppose that a gravitating body with mass M and luminosity L is placed in a flow, of which velocity at the infinite upstream is v_∞ and of which density is ρ_∞ . If the velocity v_∞ is much larger than the sound speed c_∞ of the gas at infinity (or if the Mach number of the upstream flow is much larger than unity), then the pressure effect can be neglected except for the very center. If we compare the kinetic energy of the gas, $v_\infty^2/2$, with the potential energy of the gas, GM/r , we obtain the *Hoyle-Lyttleton accretion radius* R_{HL} :

$$R_{\text{HL}} = \frac{2GM}{v_\infty^2} \quad (1)$$

(More precisely, the accretion radius is derived from the escape condition on the accretion axis, as described later). Inside the accretion radius the potential energy exceeds the kinetic energy and the gas is trapped by the gravitating object. By a simple argument, Hoyle and Lyttleton (1939) showed that a gas with the impact parameter less than R_{HL} accretes onto the gravitating body. Thus, the rate of mass accretion, \dot{M}_{HL} , on to the gravitating object is

$$\dot{M}_{\text{HL}} = \pi R_{\text{HL}}^2 \rho_\infty v_\infty = \frac{4\pi \rho_\infty G^2 M^2}{v_\infty^3}. \quad (2)$$

If we know the accretion rate, we can estimate the (accretion) luminosity of the radiation emitted from the compact object. Therefore, the knowledge on the accretion radius is important to compare theories with observations.

Bondi (1952) considered a spherical accretion and obtained the so-called Bondi radius R_B :

$$R_B = \frac{GM}{c_\infty^2}, \quad (3)$$

where c_∞ is the sound speed of gas at infinity. Hence, if we take account of the gas pressure, the accretion radius and accretion rate are modified respectively as

$$R_{\text{HLB}} = \frac{2GM}{v_\infty^2 + c_\infty^2}, \quad (4)$$

$$\dot{M}_{\text{HLB}} = \frac{4\pi\rho_\infty G^2 M^2}{(v_\infty^2 + c_\infty^2)^{3/2}}, \quad (5)$$

considering the results of numerical simulations (Bondi 1952; Shima et al. 1985).

Later, Taam et al. (1991) took into account the effect of the radiation pressure force, and obtained the accretion radius modified by the radiation pressure:

$$R_{\text{HL}}^R = \frac{2GM(1 - \Gamma)}{v_\infty^2}, \quad (6)$$

when the gas is fully ionized and transparent. Here, Γ is the indication of luminosity strength, i.e., the ratio of the luminosity L of the gravitating object to the Eddington luminosity $L_E (= 4\pi cGMm_p/\sigma_T)$:

$$\Gamma = \frac{L}{L_E}, \quad (7)$$

where m_p is the proton mass and σ_T the Thomson scattering cross-section. The reason, why the effect of radiation pressure is expressed by such a simple formula as equation (6), is because the radiation pressure decreases as r^{-2} , which is the same dependence as that of gravity. The formula (6) means the following facts: (i) If the luminosity of the gravitating object is sub-Eddington, the accretion radius reduces by a factor $(1 - \Gamma)$ compared with the Hoyle-Lyttleton radius. (ii) If the luminosity is super-Eddington, the accretion cannot take place and the gas particles will be scattered by the radiation pressure (the radiative Rutherford scattering).

2.2. Radiation Fields of the Central Source

Let us assume that the luminous gravitating object is located at the origin, and it is immersed in the uniform gas flow. The total luminosity of the central object is L . We also assume that the gas is fully ionized and transparent to the radiation from the object. We adopt the cylindrical coordinates (r, φ, z) , where the z -axis is in the direction of the gas particle at the upstream.

At a point whose radial distance from the central object is $R (= \sqrt{r^2 + z^2})$, the radiation energy density E , the radiative flux F^R in the R -direction, and the diagonal component of the radiation stress tensor P^{RR} are expressed respectively as

$$E = \frac{F^R}{c} = \frac{1}{c} \frac{L}{4\pi R^2}, \quad (8)$$

$$F^R = \frac{L}{4\pi R^2}, \quad (9)$$

$$P^{RR} = E = \frac{1}{c} \frac{L}{4\pi R^2}, \quad (10)$$

in the region where the central object is treated as a point source (other components vanish). It should be noted that if the effect of the finite source size is taken into account, the radiation energy density is enhanced in the very vicinity of the central object (Guess 1962; Carroll 1990).

2.3. Basic Equations

In order to make the problem tractable, let us assume that the flow is axisymmetric about the axis penetrating the center of the gravitating body and parallel to the incident flow (accretion axis). We neglect the gas pressure, the viscosity, the heating, the cooling, and the magnetic field.

The motion of the gas particle in the radiation fields is described by

$$\frac{d\mathbf{v}}{dt} = -\nabla\phi + \frac{\sigma_{\text{T}}}{mc}(\mathbf{F} - E\mathbf{v} - \mathbf{P} \otimes \mathbf{v}), \quad (11)$$

upto the first order of v/c , where \mathbf{v} is the particle velocity, ϕ the gravitational potential, m the particle mass (proton mass for the normal plasma), E the radiation energy density, \mathbf{F} the radiative flux vector, and \mathbf{P} the radiation stress tensor (Hsieh, Spiegel 1976; Fukue et al. 1985; see also Kato et al. 1998). The terms $(-E\mathbf{v} - \mathbf{P} \otimes \mathbf{v})$ express the radiation drag force, which is our main concern in the present paper.

In the cylindrical coordinates (r, φ, z) , the equation (11) is expressed as

$$\frac{dv_r}{dt} = -\frac{GMr}{R^3} + \frac{\sigma_{\text{T}}}{mc} \left[F^R \frac{r}{R} - Ev_r - P^{RR} \frac{r}{R} \left(v_r \frac{r}{R} + v_z \frac{z}{R} \right) \right], \quad (12a)$$

$$\frac{dv_z}{dt} = -\frac{GMz}{R^3} + \frac{\sigma_{\text{T}}}{mc} \left[F^R \frac{z}{R} - Ev_z - P^{RR} \frac{z}{R} \left(v_r \frac{r}{R} + v_z \frac{z}{R} \right) \right], \quad (12b)$$

retaining the non-zero components of radiation fields. Let us normalize the length and the time by r_g and r_g/c , respectively, where r_g is the Schwarzschild radius of the central object. Substituting the expressions for E , F^R , and P^{RR} , and normalizing the resultant equations, we finally have the following equations:

$$\frac{dv_r}{dt} = -\frac{(1-\Gamma)r}{2R^3} - \frac{\Gamma}{2R^2} \left[\left(1 + \frac{r^2}{R^2} \right) v_r + \frac{rz}{R^2} v_z \right], \quad (13a)$$

$$\frac{dv_z}{dt} = -\frac{(1-\Gamma)z}{2R^3} - \frac{\Gamma}{2R^2} \left[\frac{rz}{R^2} v_r + \left(1 + \frac{z^2}{R^2} \right) v_z \right]. \quad (13b)$$

Here, the symbols for the dimensionless variables, say “ \hat{v} ”, are dropped.

There are two physical parameters defining the problem: v_{∞} and Γ . We consider the following three cases:

- Case A: If we set Γ to be zero, we obtain the equations of ballistic orbits of a particle mass. This is just the original Hoyle-Lyttleton accretion.
- Case B: If we neglect the second terms of the right-hand sides of equations (13), then we obtain the equations of motion of a particle in which only the gravity and the radiation pressure are taken into account. This is the case examined by, e.g., Taam et al. (1991).
- Case C: If we take into account all the terms in equations (13), we obtain the equations of motion of a particle which is affected not only by the gravity and the radiation pressure but also radiation drag.

3. Results

3.1. Particle Trajectory

We first calculate trajectories of particles by integrating equation (13) using the forth-order Runge-Kutta-Gill method. In cases A and B, as is well known, particle trajectories are hyperbolae. The equation of hyperbolic orbits in the polar coordinates is $r = \ell/(1 + \varepsilon \cos \theta)$, where $\ell = b^2 v_\infty^2/[GM(1 - \Gamma)]$ and $\varepsilon = \sqrt{1 + b^2 v_\infty^4/[G^2 M^2 (1 - \Gamma)^2]}$, b being the impact parameter. In order to compare the present case C with cases A and B, and to check the numerical accuracy, we show the numerical results of all cases.

Figure 1 show the trajetories of gas particles in the case of $v_\infty = 0.1c$ for several Γ ; $\Gamma = 0$ in figure 1a (i.e., the central object does not emit radiation), $\Gamma = 0.5$ in figure 1b, $\Gamma = 1.0$ in figure 1c (i.e., the luminosity of the central object is the Eddington one), and $\Gamma = 1.2$ in figure 1d. Short-dashed curves are for case A (gravity only), chain-dotted ones for case B (gravity and radiation pressure), and solid ones for case C (including radiation drag).

In figure 1b (sub-Eddington luminosity) we see the example where a particle accretes to the central object if radiation drag is included, otherwise a particle can escape.

In figure 1c (Eddington luminosity) the trajectories of particles in cases B and C are almost straight lines, since the effect of gravity is canceled by the radiation pressure. Precisely speaking, in case B the trajectory is exactly straight, while it slightly deviates from the straight line in case C. This is understood as follows. In case C including radiation drag, a particle initially moves in the z -direction and does not move in the r -direction so that there is no radiation drag force originating from the radiation energy density E . However, there exists the radiation drag force arising from the radiation stress tensor P^{RR} [see equation (13)], since P^{RR} interacts with v_z . As a result, there appears a residual (positive) force in the r -direction for $v_z < 0$. This is the case of the trajectory in case C.

In figure 1d (super-Eddington luminosity) the particles in cases B and C are expelled due to the radiation pressure (this is just the *radiative Rutherford scattering*). In case C with radiation drag, the “scattering” is apparently strong compared with that of case B. This is understood as follows. In case C the particle motion in the z -direction is suppressed by the effect of radiation drag, and the vertical velocity v_z becomes slow. As a result, the trajectory in case C becomes similar to the one in case B, which is “compressed” in the z -direction.

Figure 1

3.2. Accretion Radius

We calculate the accretion radius by the almost same procedure as Hoyle and Lyttleton (1939). Let us suppose that two particles intersecting downstream on the accretion axis collide and lose their transverse momenta. If the resultant z -velocity is less than the escape velocity at that point, these particles are assumed to be captured and accreted on the gravitating body. In case C, however, more sophisticated treatment is necessary. During the coalesced particle moves on the accretion axis after collision, it is suffered from radiation drag and loses its z -momentum. Thus, in order to determine the accretion radius, we follows the particle motion on the accretion axis whether it escapes or turns to infall toward the center in case C.

Figure 2 shows the accretion radius R_{acc} normalized by the Hoyle-Lyttleton accretion radius R_{HL} ($= 2GM/v_\infty^2$) as a function of the normalized luminosity Γ ($= L/L_E$) in the case of $v_\infty = 0.1c$. As can be seen from figure 2, for case A (short-dashed line) the normalized accretion radius $R_{\text{acc}}/R_{\text{HL}}$ is always unity, since this is nothing but the original Hoyle-Lyttleton accretion ($R_{\text{acc}} = R_{\text{HL}}$). In case B (chain-dotted line) $R_{\text{acc}}/R_{\text{HL}}$ is a liner function of Γ and it vanishes at $\Gamma = 1$ [$R_{\text{acc}} = R_{\text{HL}}^R = (1 - \Gamma)R_{\text{HL}}$]. Case C (solid curve) shows our present result. The calculated $R_{\text{acc}}/R_{\text{HL}}$ in case C lies between those of cases A and B. That is, the

effect of radiation drag increases the accretion radius for case B without radiation drag. The solid curve is the case where the particle motion on the accretion axis is followed, as stated above, while the dashed one is the case where the condition of accretion is determined by the escape condition like cases A and B. As is expected, the effect of radiation drag on coalesed particles slightly increases the accretion radius.

Figure 3 shows the accretion radius for several cases of incident velocities v_∞ . As can be seen in figure 3, the effect of radiation drag becomes more important for a higher incident velocity as large as $0.3c$. The effect of radiation drag almost cancels the outward radiation pressure, if Γ is not so large.

Figures 2-3

We here derive the analytical approximate formula expressing the accretion radius for the case of small v . If we restrict ourselves in the R -direction and use v instead of v_R , equation (11) becomes

$$\frac{dv}{dt} = -\frac{GM}{R^2} + \frac{\sigma_T}{mc} (F^R - 2Ev) = -\frac{GM(1-\Gamma)}{R^2} - \frac{GM}{R^2} 2\Gamma \frac{v}{c}. \quad (14)$$

The energy integration of this equation roughly gives the following expression:

$$\frac{1}{2}v_\infty^2 \sim \frac{GM(1-\Gamma)}{R_{\text{acc}}} + \frac{GM}{R_{\text{acc}}} 2\Gamma \frac{v_\infty}{c}. \quad (15)$$

Hence, the accretion radius under radiation drag is roughly expressed as

$$\frac{R_{\text{acc}}}{R_{\text{HL}}} \sim 1 - \Gamma \left(1 - \frac{2v_\infty}{c} \right). \quad (16)$$

This formula (16) well reproduces the results shown in figures 2-3 in the limit of small v , and clearly shows the effects of radiation pressure and drag; i.e., Γ reduces R_{acc} while v_∞ increases R_{acc} .

4. Concluding Remarks

We conclude that the accretion radius becomes larger, if we take into account of radiation drag, compared with the case in which only the effect of radiation pressure is taken into account. The present effect becomes prominent when the incident velocity of gas is comparable to the speed of light, and the luminosity of the central object is comparable to the Eddington luminosity.

In the present paper we bear in mind the Compton drag in highly ionized media (normal plasmas as well as electron-positron pair plasmas). The result, however, is applicable to more general cases including dust, as long as the gray approximation is valid. That is, the effect of radiation drag becomes important if the specific cross-section of particles (“opacity”) is sufficiently large.

We assume that the media is transparent. In the hydrodynamical accretion, however, the optical depth of the media should be considered. For roughly uniform media, the optical depth exceeds unity beyond some critical radius. Hence, radiation drag as well as radiation pressure effectively operate inside some radius.

In this paper we consider the mildly relativistic case, where the equations are of the first order of v/c . In the case where the incident velocity is much close to c , higher order terms should be included and we must treat the problem within the framework of full special relativity. In addition if the velocity is of the order of c , the accretion radius becomes of the order of r_g , or the central source size for compact objects. In such a situation

the effect of the finite source size cannot be neglected. In some cases the general relativistic effect becomes non-negligible. These are left as a future work.

Reference

- Bondi H. 1952, MNRAS 112, 195
Bondi H., Hoyle F. 1944, MNRAS 104, 273
Carroll D.L. 1990, ApJ 348, 588
Davis R.E., Pringle J.E. 1980, MNRAS 191, 599
Fortner B., Lamb F.K., Miller G.S. 1989, Nature 342, 775
Fryxell B.A., Taam R.E., McMillan S.L.W. 1987, ApJ 315, 536
Fukue J., Kato S., Matsumoto R. 1985, PASJ 37, 383
Fukue J., Umemura M. 1995, PASJ 47, 429
Guess A.W. 1962, ApJ 135, 855
Ho C., Taam R.E., Fryxell B.A., Matsuda T., Koide H., Shima E. 1989, MNRAS 238, 1447
Hoyle F., Lyttleton R.A. 1939, Proc. Camb. Phil. Soc. 35, 405
Hsieh S.-H., Spiegel E.A. 1976, ApJ 207, 244
Hunt R. 1971, MNRAS 154, 141
Kato S., Inagaki S., Fukue J., Mineshige S. (eds) 1996, Basic Physics of Accretion Disks (Gordon Breach, New York)
Kato S., Fukue J., Mineshige S. 1998, Black-Hole Accretion Disks (Kyoto University Press, Kyoto)
Koide H., Matsuda T., Shima E. 1991, MNRAS 252, 473
Meyer F., Meyer-Hofmeister E. 1994, A&Ap 288, 175
Poynting J.H. 1903, Phil Trans R Soc London, Ser A 202, 525
Robertson H.P. 1937, MNRAS 97, 423
Shima E., Matsuda T., Takeda H., Sawada K. 1985, MNRAS 217, 367
Taam R.E., Fu A., Fryxell B.A. 1991, ApJ 371, 696
Tajima Y., Fukue J. 1996, PASJ 48, 529
Treves A., Maraschi L., Abramowicz M. 1988, PASP 100, 427
Watanabe Y., Fukue J. 1996, PASJ 48, 849

Figure Captions

Fig. 1. Examples of particle trajectories in the case of $v_\infty = 0.1c$ for several values of Γ . The values of Γ are (a) 0, (b) 0.5, (c) 1.0, and (d) 1.2. The abscissae are r , whereas the ordinates are z , both in units of r_g . Particles, coming from upward initially, are captured or scattered due to the effects of gravity only (case A; short-dashed curves), gravity and radiation pressure (case B; chain-dotted curves), and gravity, radiation pressure, and radiation drag (case C; solid curves).

Fig. 2. Accretion radius normalized by the Hoyle-Lyttleton one, $R_{\text{acc}}/R_{\text{HL}}$, as a function of the normalized luminosity Γ . The short-dashed horizontal line indicates case A, where only the gravity is included. The chain-dotted line, which linearly decreases with Γ , expresses case B, where the radiation pressure as well as gravity are included. The thick solid curve shows case C, the present result under the effect of radiation drag. The dashed curve also shows case C, where the condition of accretion is determined by the escape condition like cases A and B.

Fig.3. Accretion radius for several values of incident velocity v_∞ .

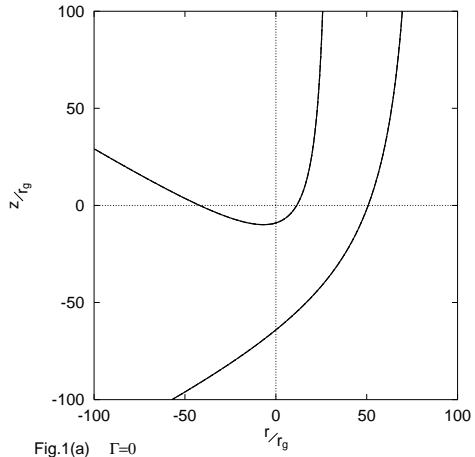


Fig.1(a) $\Gamma=0$

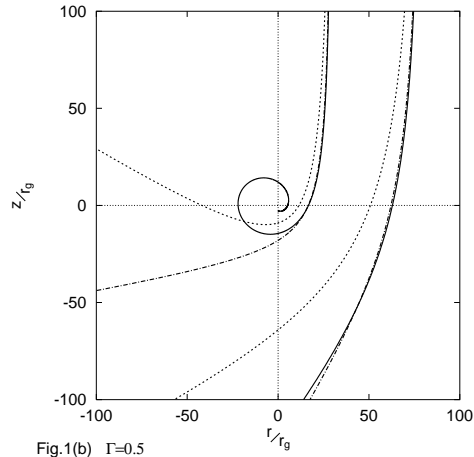


Fig.1(b) $\Gamma=0.5$

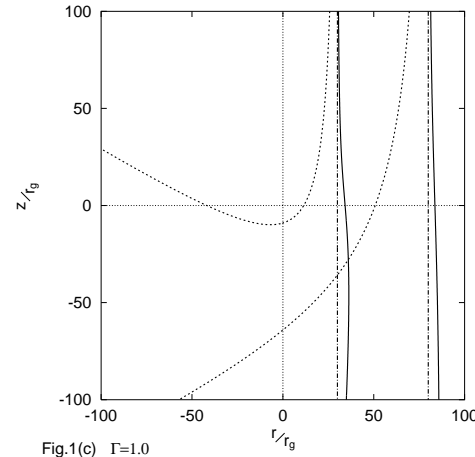


Fig.1(c) $\Gamma=1.0$

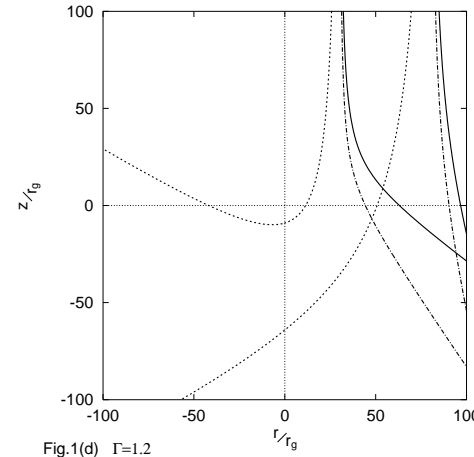


Fig.1(d) $\Gamma=1.2$

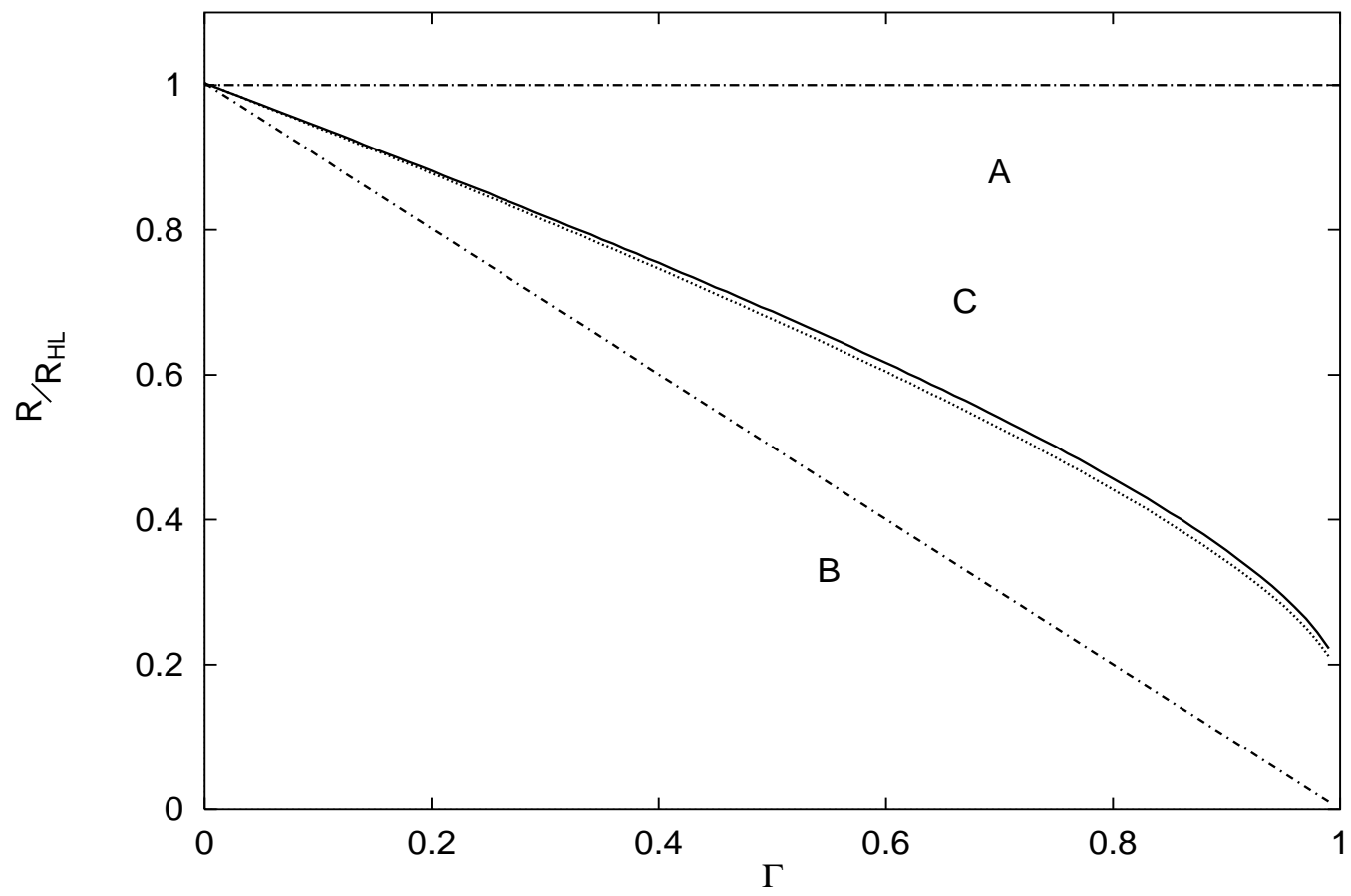


Fig.2.

Π

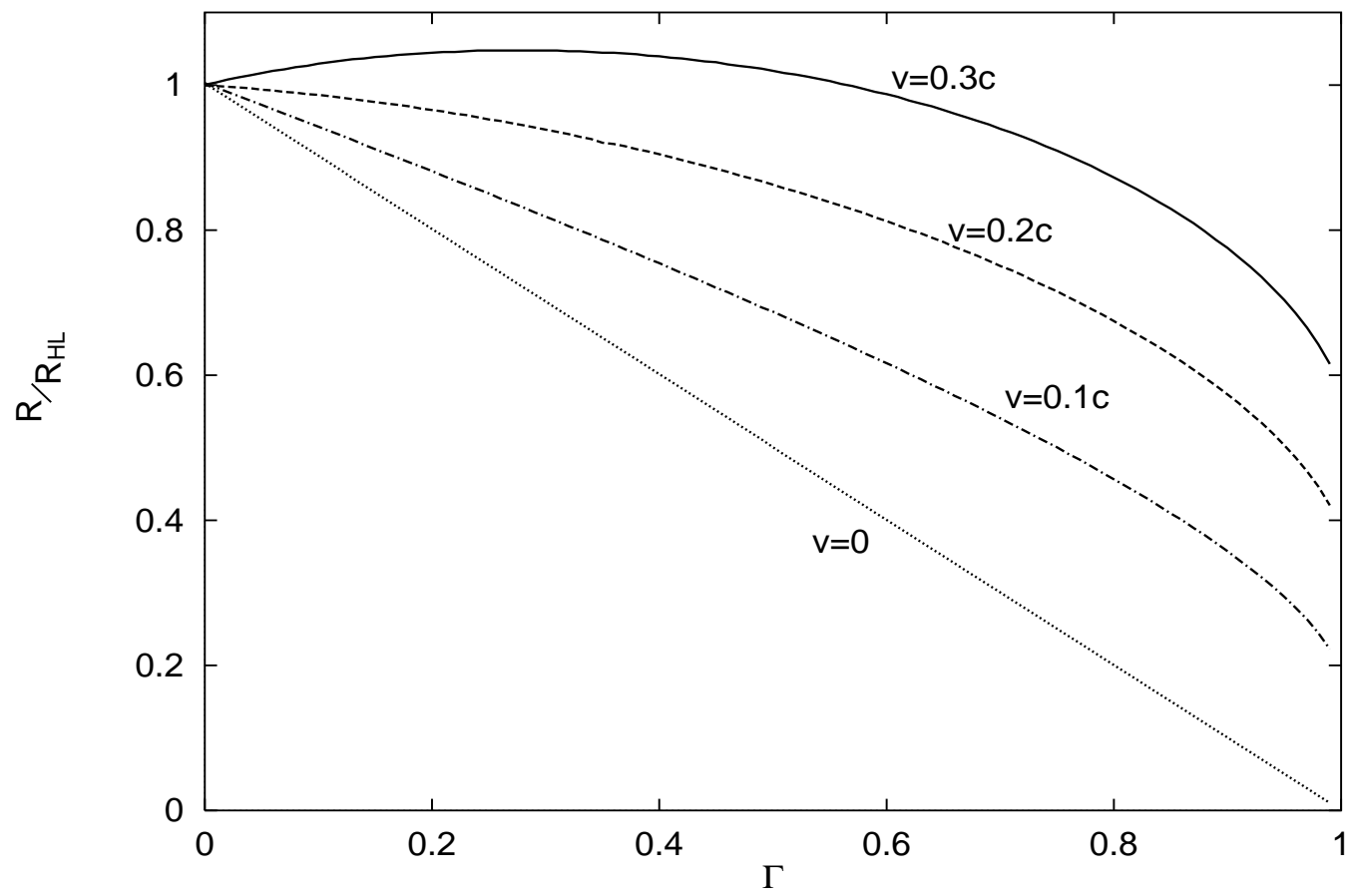


Fig.3.